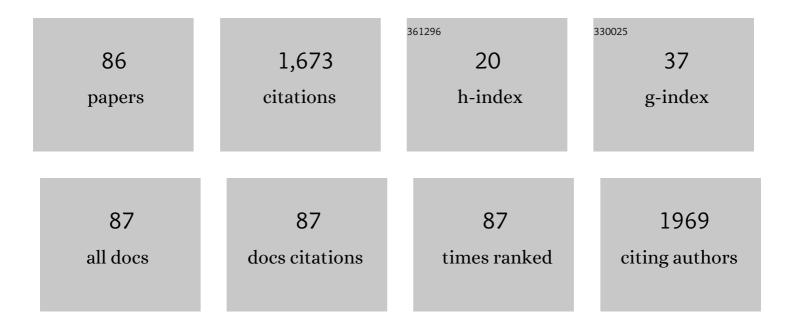
## Ge-Mei Cai

List of Publications by Year in descending order

Source: https://exaly.com/author-pdf/1938782/publications.pdf Version: 2024-02-01



CE-MELCAL

#	Article	IF	CITATIONS
1	Synthesis of Mo2N nanolayer coated MoO2 hollow nanostructures as high-performance anode materials for lithium-ion batteries. Energy and Environmental Science, 2013, 6, 2691.	15.6	246
2	The Non-Concentration-Quenching Phosphor Ca <sub>3</sub> Eu <sub>2</sub> B <sub>4</sub> O <sub>12</sub> for WLED Application. Inorganic Chemistry, 2020, 59, 3894-3904.	1.9	118
3	New Prelithiated V <sub>2</sub> O <sub>5</sub> Superstructure for Lithium-Ion Batteries with Long Cycle Life and High Power. ACS Energy Letters, 2020, 5, 31-38.	8.8	113
4	Tuning of Emission by Eu <sup>3+</sup> Concentration in a Pyrophosphate: the Effect of Local Symmetry. Inorganic Chemistry, 2020, 59, 2241-2247.	1.9	78
5	Structure, luminescence and energy transfer in Ce <sup>3+</sup> and Mn <sup>2+</sup> codoped γ-AlON phosphors. Journal of Materials Chemistry C, 2019, 7, 733-742.	2.7	66
6	Layered Crystal Structure, Color-Tunable Photoluminescence, and Excellent Thermal Stability of MgIn <sub>2</sub> P <sub>4</sub> O <sub>14</sub> Phosphate-Based Phosphors. Inorganic Chemistry, 2017, 56, 12902-12913.	1.9	61
7	Measurement of interdiffusion and impurity diffusion coefficients in the bcc phase of the Ti–X (XÂ=ÂCr,) Tj E 3255-3268.	「Qq1 1 0.7 1.7	84314 rgBT 50
8	Single-phased and color tunable LiSrBO 3 :Dy 3+ , Tm 3+ , Eu 3+ phosphors for white-light-emitting application. Journal of Luminescence, 2017, 187, 211-220.	1.5	47
9	Efficient and stable Sr <sub>3</sub> Eu <sub>2</sub> B <sub>4</sub> O <sub>12</sub> red phosphor benefiting from low symmetry and distorted local environment. Dalton Transactions, 2020, 49, 3260-3271.	1.6	36
10	New promising phosphors Ba3InB9O18 activated by Eu3+/Tb3+. Journal of Luminescence, 2010, 130, 910-916.	1.5	31
11	Tunable luminescence properties and energy transfer of Tm3+, Dy3+, and Eu3+ co-activated InNbO4 phosphors for warm-white-lighting. Ceramics International, 2016, 42, 15994-16006.	2.3	30
12	Daylight-White-Emitting and Abnormal Thermal Antiquenching Phosphors Based on a Layered Host Srln <sub>2</sub> (P <sub>2</sub> O <sub>7</sub> ) <sub>2</sub> . Inorganic Chemistry, 2021, 60, 2279-2293.	1.9	30
13	A new promising scintillator Ba3InB9O18. Journal of Solid State Chemistry, 2008, 181, 646-651.	1.4	29
14	Structure and luminescence properties of multicolor phosphors with excellent thermal stability based on a new phosphate Ba3In4(PO4)6. Journal of Alloys and Compounds, 2019, 797, 775-785.	2.8	29
15	Crystal structure, luminescence properties and energy transfer of Eu <sup>3+</sup> /Dy <sup>3+</sup> doped GdNbTiO <sub>6</sub> broad band excited phosphors. RSC Advances, 2016, 6, 50797-50807.	1.7	28
16	Insight into crystal structure and Eu/Tb doped luminescence property of a new phosphate. Journal of Alloys and Compounds, 2018, 762, 444-455.	2.8	26
17	Controlling spin-dependent tunneling by bandgap tuning in epitaxial rocksalt MgZnO films. Scientific Reports, 2014, 4, 7277.	1.6	24
18	Structure, tunable luminescence and thermal stability in Tb3+ and Eu3+ co-doped novel KBaIn2(PO4)3 phosphors. Journal of Luminescence, 2020, 221, 117115.	1.5	23

#	Article	IF	CITATIONS
19	Tunable emission, energy transfer and thermal stability of Ce3+, Tb3+ co-doped Na2BaCa(PO4)2 phosphors. Journal of Rare Earths, 2022, 40, 878-887.	2.5	23
20	Investigation on Eu/Tb activated photoluminescent properties of Li 3 Sc(BO 3 ) 2 based phosphors. Journal of Alloys and Compounds, 2017, 719, 171-181.	2.8	20
21	Structure and luminescent properties of new Dy3+/Eu3+/Sm3+-activated InNbTiO6 phosphors for white UV-LEDs. Optical Materials, 2019, 98, 109403.	1.7	20
22	Experimental investigation of phase equilibria in the Ti–Al–Mo ternary system. Journal of Materials Science, 2017, 52, 2270-2284.	1.7	18
23	Dependence of Luminous Performance on Eu <sup>3+</sup> Site Occupation in Srln <sub>2</sub> (P <sub>2</sub> O <sub>7</sub> ) <sub>2</sub> : The Effect of the Local Environment. Inorganic Chemistry, 2021, 60, 17219-17229.	1.9	18
24	Three-dimensional FeSe2 microflowers assembled by nanosheets: Synthesis, optical properties, and catalytic activity for the hydrogen evolution reaction. Electronic Materials Letters, 2016, 12, 237-242.	1.0	17
25	Investigation of the phase equilibria in Ti-Ni-Hf system using diffusion triples and equilibrated alloys. Calphad: Computer Coupling of Phase Diagrams and Thermochemistry, 2017, 58, 160-168.	0.7	16
26	Measurement of Diffusion Coefficients in the bcc Phase of the Ti-Sn and Zr-Sn Binary Systems. Metallurgical and Materials Transactions A: Physical Metallurgy and Materials Science, 2019, 50, 1409-1420.	1.1	16
27	Realizing high thermoelectric performance in Cu <sub>2</sub> Te alloyed Cu <sub>1.15</sub> In <sub>2.29</sub> Te <sub>4</sub> . Journal of Materials Chemistry A, 2019, 7, 2360-2367.	5.2	16
28	Regular hexagonal MoS2 microflakes grown from MoO3 precursor. Applied Physics A: Materials Science and Processing, 2007, 89, 783-788.	1.1	15
29	Crystal structure and Eu3+/Tb3+ doped luminescent properties of a new borate Ba3BiB9O18. Materials Research Bulletin, 2009, 44, 2211-2216.	2.7	15
30	Red-green-blue-tunable emission from Eu3+ and Tb3+ codoped pyrophosphate phosphors. Journal of Luminescence, 2019, 215, 116732.	1.5	15
31	Large optical polarizability causing positive effects on the birefringence of planar-triangular BO <sub>3</sub> groups in ternary borates. Dalton Transactions, 2020, 49, 3284-3292.	1.6	15
32	Synthesis and relative optical properties of Eu3+/Tb3+-activated Li3InB2O6. Journal of Alloys and Compounds, 2013, 562, 182-186.	2.8	14
33	A peculiar layered 12-fold cationic coordination compound LiInTi <sub>2</sub> O <sub>6</sub> : phase relations, crystal structure and color-tunable photoluminescence. RSC Advances, 2017, 7, 22156-22169.	1.7	13
34	Thermodynamic investigation of the Mg-Ni-Zn system by experiments and calculations and its application. Journal of Alloys and Compounds, 2019, 784, 769-787.	2.8	13
35	Photoluminescence and energy transfer of efficient and thermally stable white-emitting Ca9La(PO4)7:Ce3+, Tb3+, Mn2+ phosphors. Ceramics International, 2021, 47, 12056-12065.	2.3	13
36	Crystal structure and luminescence properties of a novel promising phosphor Ba <sub>3</sub> ScB <sub>9</sub> O <sub>18</sub> . Powder Diffraction, 2007, 22, 328-333.	0.4	12

#	Article	IF	CITATIONS
37	Crystal structure and photoluminescence of Tb3+-activated Ba3InB3O9. Materials Chemistry and Physics, 2011, 129, 761-768.	2.0	12
38	Subsolidus phase relations in CaO–In2O3–B2O3 system and crystal structure of CaInBO4. Journal of Alloys and Compounds, 2012, 516, 107-112.	2.8	11
39	Luminescent properties and performance tune of novel red-emitting phosphor CalnBO4: Eu3+. Journal of Alloys and Compounds, 2015, 650, 494-501.	2.8	11
40	Investigation of phase equilibria in the Ti-Co-Zr ternary system. Calphad: Computer Coupling of Phase Diagrams and Thermochemistry, 2017, 56, 260-269.	0.7	11
41	Synthesis and photoluminescence of host-sensitized MgNb2O6 based phosphors. Journal of Luminescence, 2018, 198, 10-18.	1.5	11
42	Multicolor emission leading by energy transfer between Dy3+ and Eu3+ in wolframite InNbTiO6. Journal of Luminescence, 2020, 227, 117578.	1.5	11
43	Excellent enhancement of thermal stability and quantum efficiency for Na2BaCa(PO4)2:Eu2+ phosphor based on Sr doping into Ca. Journal of Alloys and Compounds, 2022, 911, 165092.	2.8	11
44	Synthesis, crystal structure, and thermal stability of new borates Na <sub>3</sub> REB <sub>2</sub> O <sub>6</sub> (RE = Pr, Sm, Eu). Powder Diffraction, 2016, 31, 110-117.	0.4	10
45	Significant improvement in the thermoelectric performance of Sb-incorporated chalcopyrite compounds Cu <sub>18</sub> Ga <sub>25</sub> Sb <sub>x</sub> Te <sub>50â<sup>°</sup>x</sub> ( <i>x</i> = 0–3.125) through the coordination of energy band and crystal structures. Journal of Materials Chemistry A, 2017. 5. 24199-24207.	5.2	10
46	Structure, tunable luminescence and energy transfer in Tb <sup>3+</sup> and Eu <sup>3+</sup> codoped Ba <sub>3</sub> InB <sub>9</sub> O <sub>18</sub> phosphors. RSC Advances, 2019, 9, 1029-1035.	1.7	10
47	Structure and tunable luminescence in Sm3+/Er3+ doped host-sensitized LaNbO4 phosphor by energy transfer. Ceramics International, 2020, 46, 28373-28381.	2.3	10
48	Enhanced scintillation of Ba3In(B3O6)3 based on nitrogen doping. Journal of Solid State Chemistry, 2018, 258, 351-357.	1.4	9
49	Reduction of Ce(IV) to Ce(III) induced by structural characteristics and performance characterization of pyrophosphate MgIn2P4O14-based phosphors. Journal of Luminescence, 2018, 203, 590-598.	1.5	9
50	Review of Heteroleptic Tetrahedra as Birefringent or Nonlinear Optical Motifs. Crystal Growth and Design, 2022, 22, 1500-1514.	1.4	9
51	Room temperature luminescence and ferromagnetism of AlN:Fe. AIP Advances, 2016, 6, 065025.	0.6	8
52	Experimental investigation on phase equilibria of Cu–Ti–Hf system and performance of Cu(Ti, Hf)2 phase. Journal of Materials Science, 2018, 53, 7809-7821.	1.7	8
53	Enhanced thermoelectric properties in N-type Mg <sub>2</sub> Si <sub>0.4â^'x</sub> Sn <sub>0.6</sub> Sb <sub>x</sub> synthesized by alkaline earth metal reduction. RSC Advances, 2019, 9, 4008-4014.	1.7	8
54	Screening Nitrides with High Debye Temperatures as Nonlinear Optical Materials. Journal of Physical Chemistry C, 2022, 126, 7047-7053.	1.5	8

#	Article	IF	CITATIONS
55	Phase relation, structure, and properties of borate MgYB <sub>5</sub> O <sub>10</sub> in MgO–Y <sub>2</sub> O <sub>3</sub> –B <sub>2</sub> O <sub>3</sub> system. Powder Diffraction, 2017, 32, 97-106.	0.4	7
56	Experimental investigation and thermodynamic calculation of Ti-Co-Hf system. Calphad: Computer Coupling of Phase Diagrams and Thermochemistry, 2018, 62, 128-140.	0.7	7
57	The triâ€emitting phosphate phosphors SrIn <sub>2</sub> (P <sub>2</sub> O <sub>7</sub> ) <sub>2</sub> : Tm, Dy, Eu for ratiometric optical thermometer. Journal of the American Ceramic Society, 2022, 105, 6184-6195.	1.9	7
58	Modification of YNbO4 and YNbTiO6 photoluminescence by nitrogen doping. AIP Advances, 2018, 8, .	0.6	6
59	Synergistic Regulation of Phonon and Electronic Properties to Improve the Thermoelectric Performance of Chalcogenide Culn <sub>1â^'</sub> <i><sub>x</sub></i> Ga <i><sub>x</sub></i> Te <sub>2</sub> : <i>y</i> InTe ( <i>x</i> =) Tj ET	- <del>Ç</del> iq1 1 0.	784314 rg <sup>B</sup>
60	Synthesis of Euâ€doped hydroxyapatite whiskers and fabrication of phosphor layer via electrophoretic deposition process. Journal of the American Ceramic Society, 2020, 103, 6780-6792.	1.9	6
61	Phase relation and transition in the Ti-Al-Mn system. Journal of Alloys and Compounds, 2021, 861, 158578.	2.8	6
62	Enhancement of Eu2+ photoluminescence behavior in NaBaB9O15 based on the K+ doping. Journal of Luminescence, 2022, 243, 118613.	1.5	6
63	Crystal structure determination of new compounds Li <sub>6</sub> <i>M</i> B <sub>3</sub> O <sub>9</sub> ( <i>M</i> =Nd,Sm,Eu,Tm,Er). Powder Diffraction, 2008, 23, 3-9.	0.4	5
64	The strategy of design and preparation for outstanding precipitation strengthened HEAs based on diffusion couple. Materials and Design, 2022, 217, 110667.	3.3	5
65	Phase relations, crystal structure, and phase transformation of In 1â^'x Nb 1â^'x Ti 2x O 4 (0Ââ‰Â x Â<Â0.45) in Ir 2 O 3 –Nb 2 O 5 –TiO 2 system. Journal of Alloys and Compounds, 2015, 651, 97-105.	<sup>1</sup> 2.8	4
66	Improvement of thermoelectric performance of copper-deficient compounds Cu <sub>2.5+Î</sub> In <sub>4.5</sub> Te <sub>8</sub> ( <i>Î</i> = 0–0.15) due to a degenerate impurity band and ultralow lattice thermal conductivity. RSC Advances, 2018, 8, 27163-27170.	1.7	4
67	Measurement of phase equilibria in Ti-Co-Ge ternary system. Journal of Alloys and Compounds, 2019, 793, 653-661.	2.8	4
68	Experimental investigation and thermodynamic calculation of Ti-Hf-Mn system. Calphad: Computer Coupling of Phase Diagrams and Thermochemistry, 2020, 70, 101776.	0.7	4
69	Structure of a new compound KBaB5O9 and photoluminescence characteristics of KBaB5O9:Eu3+. Powder Diffraction, 2007, 22, 292-294.	0.4	3
70	Experimental investigation of phase equilibria in Cu–Ge–Ti system. Journal of Alloys and Compounds, 2015, 651, 590-597.	2.8	3
71	Experimental Investigation of Phase Equilibria in the Cu-Co-Zr System. Journal of Phase Equilibria and Diffusion, 2017, 38, 855-864.	0.5	3
72	Phase equilibria and transformation in the Ti–Al–Ta system. Journal of Materials Science, 2022, 57, 2163-2179.	1.7	3

#	Article	IF	CITATIONS
73	Crystal structure and thermal properties of compound K <sub>2</sub> Zn <sub>3</sub> (P <sub>2</sub> O <sub>7</sub> ) <sub>2</sub> . Powder Diffraction, 2008, 23, 317-322.	0.4	2
74	Synthesis and characterization of powder four borate Sr <sub>3</sub> Sm <sub>2</sub> (BO <sub>3</sub> 4. Powder Diffraction, 2013, 28, 262-268.	0.4	2
75	Experimental investigation of phase equilibria in the Cu–Ni–Zr system. Journal of Materials Science, 2015, 50, 7238-7247.	1.7	2
76	Experimental Study on Phase Equilibria in Ti-Cu-Pt System. Journal of Phase Equilibria and Diffusion, 2017, 38, 466-476.	0.5	2
77	Experimental investigation of phase equilibria in the Tb-Si-Cr system. Calphad: Computer Coupling of Phase Diagrams and Thermochemistry, 2019, 65, 212-224.	0.7	2
78	An electromagnetic separation system for the enrichment of 39Ar. Review of Scientific Instruments, 2020, 91, 033309.	0.6	2
79	Status of high intensity low energy injector for Jinping underground nuclear astrophysics experiments. AIP Conference Proceedings, 2018, , .	0.3	1
80	Increased effective mass and carrier concentration responsible for the improved thermoelectric performance of the nominal compound Cu <sub>2</sub> Ga <sub>4</sub> Te <sub>7</sub> with Sb substitution for Cu. RSC Advances, 2018, 8, 21637-21643.	1.7	1
81	Experimental investigation of phase relationship in Ti–Fe-Hf ternary system. Calphad: Computer Coupling of Phase Diagrams and Thermochemistry, 2019, 67, 101669.	0.7	1
82	lon beam production with an antenna type 2.45 GHz electron cyclotron resonance ion source. Review of Scientific Instruments, 2020, 91, 023301.	0.6	1
83	Experimental Investigation of Phase Equilibria in the Cu–Cr–Ti System. Journal of Phase Equilibria and Diffusion, 2021, 42, 389-402.	0.5	1
84	Synthesis of Ni1â^'xZnxO hollow structures by a facile method. Physica E: Low-Dimensional Systems and Nanostructures, 2015, 66, 257-262.	1.3	0
85	Experimental Investigation of Phase Equilibria in Zr-Ni-Pt System. Journal of Phase Equilibria and Diffusion, 2018, 39, 301-314.	0.5	0
86	Experimental Investigation of Phase Equilibria in Ti–Zr–Ge System. Journal of Phase Equilibria and Diffusion, 2018, 39, 226-236.	0.5	0